Hindawi
Advances in Civil Engineering
Volume 2023, Article ID 5590608, 10 pages
https://doi.org/10.1155/2023/5590608

Research Article

Experimental Investigation on Jacked Pile-Sinking and Capacity-Induced Pore Pressure and Effective Radial Stress at the Pile-Clayey Soil Interface

Wang Lifeng,[1] Wang Xin,[2] Li Shiqiang,[3] Wang Jun,[3] Niu Xunlong,[3] Wang Donglei,[4,5] and Yonghong Wang[2]

[1]*Qingdao Fangshuo Construction Technology Co., Ltd, Qingdao 266000, China*
[2]*School of Civil Engineering, Qingdao University of Technology, Qingdao 266033, China*
[3]*China State Construction Zhongxin Construction Engineering Co., Ltd, Qingdao, China*
[4]*Qingdao Green Technology Geotechnical Engineering Co., Ltd, Qingdao 266033, China*
[5]*Qingdao Yongyuan Marine Technology Co., Ltd, Qingdao, China*

Correspondence should be addressed to Yonghong Wang; hong7986@163.com

Received 11 January 2023; Revised 21 March 2023; Accepted 10 April 2023; Published 15 May 2023

Academic Editor: Jianping Sun

Based on research into how static pressure piles sink in saturated cohesive soil, alterations caused by a rise in pore stress during the load process between the pile and the earth as well as the effects of a variation in valid radial thrust on the project are thoroughly studied. These changes are of great importance for the application and practice of practical projects. Microtest components are embedded on the surfaces of open and closed piles, and test research is conducted using a large-scale system and double-deck open and closed pipe piles. Finally, complete consideration is given to how variations in effective radial stress. Through this test, it was determined that as the pile's buried depth gradually grows, so do the valid radial thrust and excess pore pressure. However, the quantity of the superfluous pore water stress for a closed pile is higher than for an open pile. And the higher half has substantially lower effective radial thrust and overall surplus pore stress than the lower part does. The pile penetration depth is constant, and the value of h/L of the pile shaft is also rising, the occurrence of "lateral pressure degradation" of earth load between pile and earth is becoming increasingly prominent. The maximum ratio of the excess pore stress to the valid soil pressure between the pile and earth contact is 62.1% for an exposed pile and 52.1% for a sealed pile. At the interface, the effective radial stress is about 3.76~5.46 times that of the remaining pore water stress. Therefore, under changing pile penetration depths, the value of h/L will have an impact on the pile's and the soil's additional pore water pressure or excellent soil pressure. The test results have a significant impact on how static pressure piles are built and how bearing capacity is designed in real-world applications.

1. Introduction

The piling effect and lengthy bearing capacity of the static pressure pile are influenced by the pressure properties in saturated clay soil [1, 2]. Therefore, thrust and excess pore stress are particularly vital. And the actual radial stress of the interface is accurately measured according to a valid radial stress variation law caused by the static pile, and the loading is analyzed. This is advantageous to the thorough investigation of the physical mechanism and also the entire loading operation.

Most of the scholars use theoretical methods to study surplus pore stress and radial pressure. Theoretical research methods include: cavity inflation theory [3], strain path method [4, 5], and the method of the finite element [6]. Cao et al. [7] assumed that the soil is isotropic, and the theory of the undrained expansion of the circular hole is used to solve the pile-jacking process's variation law for the extra-pore water pressure and radial pressure. Tehrani et al. [8] showed that the pile's surface roughness and the soil's density has an impact on the soil pressure there. The abovementioned

research has important theoretical significance. At present, most studies concentrate on the variation of soil stress and extra pore stress in soil. However, the surplus stress caused by pumped piles jacking operations is significantly different. It is necessary to study the above problems in the process of jacked pile.

Indoor tests and field tests are the simplest methods to study the mechanical mechanism of static pressure pile penetration. Many domestic and foreign scholars have studied the jacked pile problem through laboratory tests and field tests. Bond and Jardine [9, 10] studied the pressure properties during the jacking operation through multi-functional test model piles. Lehane [11] tested the earth pressure in the field at the pile-soil contact and discovered how it varied with varying h/B (h is the height of the sensor from the pile end; B is the pile diameter). Hwang et al. [12] and Pestana et al. [13] survived the surplus pore stress and found that it is very small when the distance from the pile shaft exceeds 15 times the diameter. The body's ability to attenuate radial stress becomes more apparent as the length-to-diameter ratio rises. The surplus pore stress and soil stress reach their maximum when the pile end reaches the depth of the pore stress gauge and the soil stress gauge. It is evident from the above studies that most of the indoor laboratory studies are directed at sand, and there is a lack of research on the effective radial pressure. At present, most experimental studies on the interfacial stress characteristics of jacked piles do not consider the influence of opening on the increase of pore stress and radial pressure of jacked piles, and most studies only consider the pile sedimentation process. Based on the consideration of the split and closing jacked pressure pile, super-pore pressure dissipation and loading stage, based on the micro silicon piezoresistive pressure sensor test system, and force characteristics during the static stress pile are obtained. Through the development of two-tier open pipes, the pile surface hole embedded sleeve installation method is used to study hole pressure increment and radial pressure of the open and closed jacked pressure piles, which has certain engineering practical significance.

The response to valid vertical stress on the pierce stage cannot be ignored. The surplus pore stress gas expands once it is jacked, enhancing the pile-soil contact's shear strength because of the actual radial force there this will impact the pile's carrying capacity under normal working conditions. At the same time, the clay soil can more accurately mimic the real working state of the jacked piles when taking into account their practical application features, and it is essential to conduct the jacked pile pierce mechanism in the clay soil. At present, when jacking and loading clay soils, there is insufficient surplus pore and soil stress. It is very urgent to study effective radial pressure change in clay soil. Therefore, this study tests the vertical stress and surplus pore stress by implanting a special sensor to test the radial pressure and surplus pore stress. The effective radial stress in the whole process of piling and loading is the focus of the research. Many research studies are zero on sandy soil, and valid vertical stress at the interface of a jacked pile is relatively lacking for a cohesive soil foundation. Based on the clay soil, the actual radial pressure just at the stack interface during jacking and load operation is thoroughly studied. In reality, jacked piles are used in clayey soil majority, so the selection of clayey soil in indoor tests can effectively demonstrate the application effect of pipe jacking in engineering. This has complex engineering practical significance for enhancing jacked pile design and building in saturated clay regions.

2. Test of a Jacked-Up Indoor Model

2.1. Model Test Apparatus. The experiment was completed on an extensive model testing system at Qingdao University of Technology. Three components make up the bulk of the big scale model testing system: the model box, the loading system, and the data collection machinery. The model box is welded to a steel plate. The model box has a wall thickness of 6 mm, a bottom plate thickness of 14 mm, and measures 2800 mm by 2800 mm by 2000 mm overall. The front of the box, it is provided with tempered glass windows, and the model box is shown in Figure 1. A power unit and a reaction frame make up the loading system. The model box is placed on a base welded by an I-beam of 4000 mm × 4000 mm (length × width). The reaction frame is composed of four reaction force columns, two reaction force main beams, and one reaction forces a secondary beam. The power device includes a high-pressure oil pump with a large-stroke hydraulic cylinder, a panel control system, and a man-machine interface operation platform. The hydraulic cylinder is selected to have a large stroke of 1000 mm and can realize an uninterrupted static pressure penetration loading mode. The loading system is shown in Figure 2.

2.2. Soil Preparation. The clay used in this experiment was taken from a certain area in Qingdao. The soil preparation adopts the method of layered filling and compaction [14]. After the preparation of the soil is complete, the water is saturated slowly. In order to quicken the soil's consolidation, the sand is compacted to a height of 5 cm at the bottom of the model box, and it is allowed to stand for 20 days after presetting to ensure the foundation is fully consolidated. The top 30 cm of the model box is not filled with soil for testing preparation. Table 1 displays the fundamental indices of prepared clay.

2.3. Model Pile and Sensor Installation. This test has two model piles, open and closed. In order to install the sensor, a model pipe pile with two walls was created [15]. The closed-end model pile also used a double-walled model pipe pile, however, at the pile bottom, a sealed plate with the same diameter as the pile body is attached. The model pile size is based on the similarity theory principle and is determined according to factors such as the boundary dimension of the box, the actual length to diameter ratio of the reality pile. The model is built of aluminum and has stretchy properties of 72 GPa and a Poisson's ratio of 0.3. The MEMS earth sensing element, which is mounted at its entrance, can measure the circumferential stress between both the sample pile and the soil (Table 2 lists the sensor's specifications), and the sensor that is installed at the same time can measure the pressure.

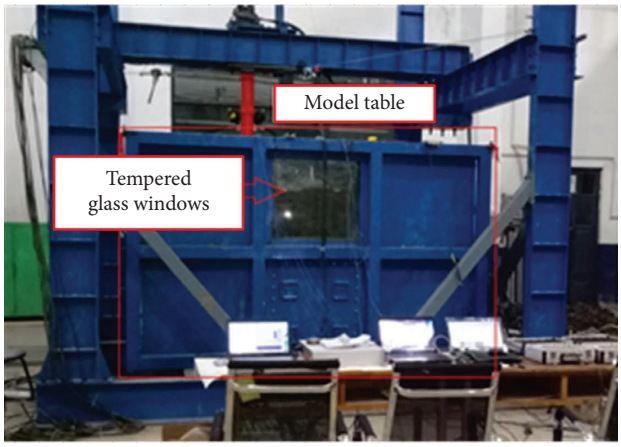

Figure 1: Model table.

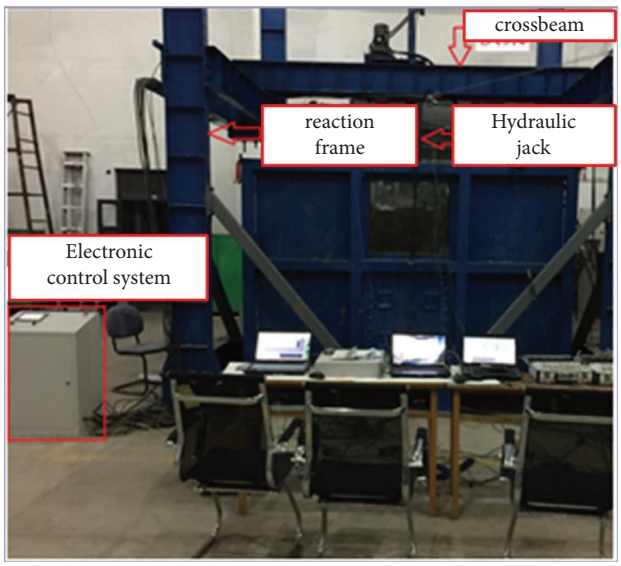

Figure 2: Loading system.

Table 1: Physical and mechanical parameters of foundation soil.

d_s	γ (kN/cm^3)	w (%)	w_L (%)	w_p (%)	I_p (%)	c (kPa)	φ (°)	$E_{s1\text{-}2}$ (MPa)
2.73	18.0	34.8	43.2	21.2	22.0	14.4	8.6	3.3

Table 2: Table of parameters for a silicon piezoresistive pressure sensor.

Species	Size (mm)	Dynamic frequency response (kHz)	Precision (%)	Operating voltage (V)
Earth pressure	20×12	2,000	0.1	0~5
Pore water pressure	20×12	2,000	0.1	0~5

Additionally, it should be mentioned that the two sensors should be installed in horizontal and constant positions, and Figure 3 illustrates how to do so. The two sensors are installed 140 mm, 280 mm, 420 mm, 560 mm, 700 mm, and 840 mm apart from one another on the pile surface. The number from bottom to top is 1#~6#, that is, to say h/L = 1, 2, 3, 4, 5, 6. The pile layout of the sensor is shown in Figure 3. In this test, the installation method of MEMS miniature silicon piezoresistive sensors is the same, both open a circular hole at the sensor installation position, weld a cylindrical sleeve at the round hole position of the inner wall, the sleeve diameter is slightly larger than the sensor diameter, fix the sensor in the sleeve through epoxy resin, and after the epoxy resin solidifies, 704 glue is coated around the sensor to protect the sensor from being damaged during the pile sinking process.

2.4. Model Test Plan. In this study, the jacked piles jacking and loading process tests of two model piles, including one open pile and one closed pile, are designed. The model test scheme is shown in Table 3. So as to fully utilize the test conditions, the model box's center is squeezed according to Figure 4. The relatively small distance between the two piles is d_1 = 1000 mm, and the model pile is d_2 = 900 mm from the nearest wall of the box, d_1/D = 7.2, d_2/D = 6.4. It complies with the pile foundation model test's requirement of 6–8 times the stake diameter for border effect [16, 17]. This model test can ignore the boundary effect. In this test, there was one loading and unloading, the depth was 900 mm, 300 mm/min was the pile jacking speed. 30 days after the completion of the jacking study, followed by a load experiment, and the loading process was carried out by grading and stepwise loading. The loading amount of each stage is set at 0.7 kN, the first stage loading is 1.4 kN, and the load of each stage is kept for 1 h. When the pile top settles, it continues to apply subsequent loads.

3. Analysis of the Study Results

3.1. Static Pressure Pile Effect

3.1.1. Analysis of the Pile-Soil Interface's Pore Water Pressure Findings. The exam TP1 and TP2 pore stress sensors' measurements as Figures 5(a) and 5(b), as test is being carried out. The pore stress at the stack interface rises roughly linearly as the depth deepens (the "depth of entry" in the text is the depth of the sensor) and is higher than the dynamic water pressure of the research soil sample, as assessed by the 1# 5# detectors at various h/L sites. This is due to the homogeneity of the soil utilized in the experiment. The mechanical characteristics close to the pile are directly impacted by the pile's burial depth. When the burial depth is shallow, the upper soil is thinner and lighter in weight compared to the lower soil, so the corresponding horizontal lateral pressure is not as great. Additionally, when the depth is shallow, pore water between the pile and soil dissipates quickly, directly reducing the water pressure therein. The pile sinking process mainly produces a crosswise distance farther from the surface of the earth, and at the same time that the lateral displacement of the ground is generated, because of the small valid stress of the soil and the vertical effective stress caused by the extrusion, it can cause the ground to rise, and soil adjacent to the pile's appearance will

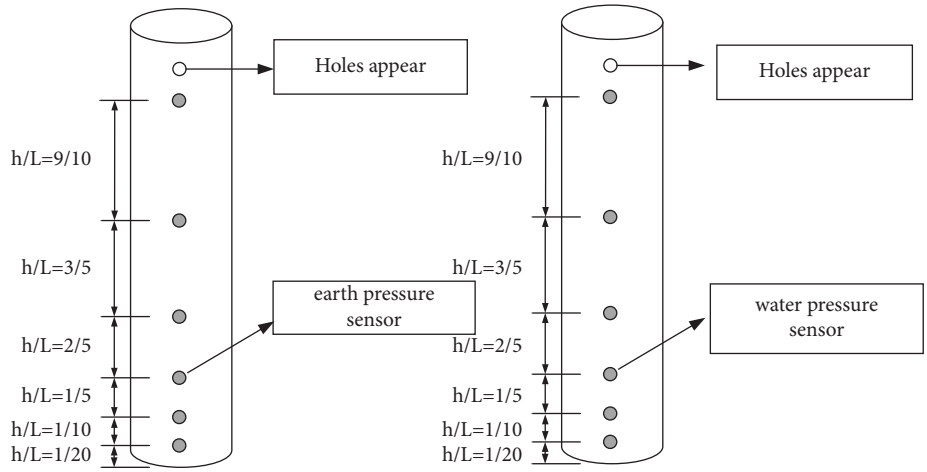

Figure 3: Soil pressure and water pressure sensors pile layout.

Table 3: Test scheme.

Test pile number	Pile length (mm)	Outer diameter (mm)	Inner diameter (mm)	Pile end form	Earth pressure sensor/number	Pore water pressure sensor/number
TP1	1,000	140	80	Open	6	6
TP2	1,000	140	80	Closed	6	6

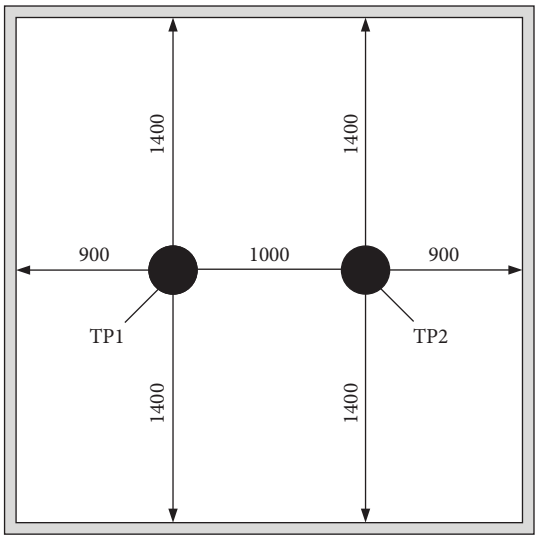

Figure 4: Layout of pile position (unit: mm).

be damaged after being disturbed, so the pore stress will quickly dissipate when buried depth is shallow. On the other hand, when the pile is buried deeply, the overburden is heavy and thick, increasing the horizontal lateral pressure proportionately. As a result, it is clear that the pile depth is directly proportional to the value of pore stress.

From Figure 5, it can also be seen that at the end of sinking, the incremental amplitudes of pore stress measured by the sensors at different h/L = 1/20, 1/10, 1/5, 2/5, and 3/5 positions of the closed test pile TP1 pile body are 12.71, 11.2, 9.35, 6.66, and 3.8 kPa, respectively. The incremental amplitudes of pore water pressure corresponding to the open test pile TP2 are 12.08, 10.68, 9.24, 6.56, and 3.87 kPa, respectively. The value of water pressure TP1 is higher than the value of TP2 when h/L is at the same height. This is due to the fact that when the pile is closed, the soil surrounding it is more compacted than when it is open, causing more soil to be deformed, which in turn causes the former's pore stress to be higher. The values of pore water pressure of 1 #5 # are quite constant when the pile's buried depth is at the same location. For instance, the largest variation in pore stress detected by 1 #5 # sensors during the sinking of the TP1 pile is just 0.32 kPa when the buried depth is 30 cm, 4.12 kPa, 4.19 kPa, 4.01 kPa, and 3.8 kPa, respectively. The pore water pressure readings for TP2 are 4.17 kPa, 4.06 kPa, 3.96 kPa, 3.73 kPa, and 3.87 kPa, with a maximum difference of about 0.3 kPa, respectively.

3.1.2. Analysis of the Pile-Soil Interface's Excessive Pore Water Pressure Results. The results of installing sensors at different h/L positions to survey pore stress and the effective soil unit weight ratio at the end of sinking are presented in Tables 4 and 5. The accompanying table shows that the ratio between the aforementioned two parameters will rise as the depth of two test heaps changes. This is mostly due to the fact that the overlying soil layer thickness and weight will be significant where the pile is deeply buried. It will have a denser. The pore stress will rise as its pierce depth rises because it will disperse water pressure more slowly. For instance, when the value of h/L is 1/20, the correlation ratio of TP2 is 52.1%, which is 9.1% different from the highest ratio of overpore stress of TP1 to valid soil weight of 61.2%. However, the closed test pile's value ought to always be higher than the open pile's. The deformation and uplift of the top soil layer are mostly to blame for this. The superpore stress caused by pile settlement is related to the valid stress of the overlying

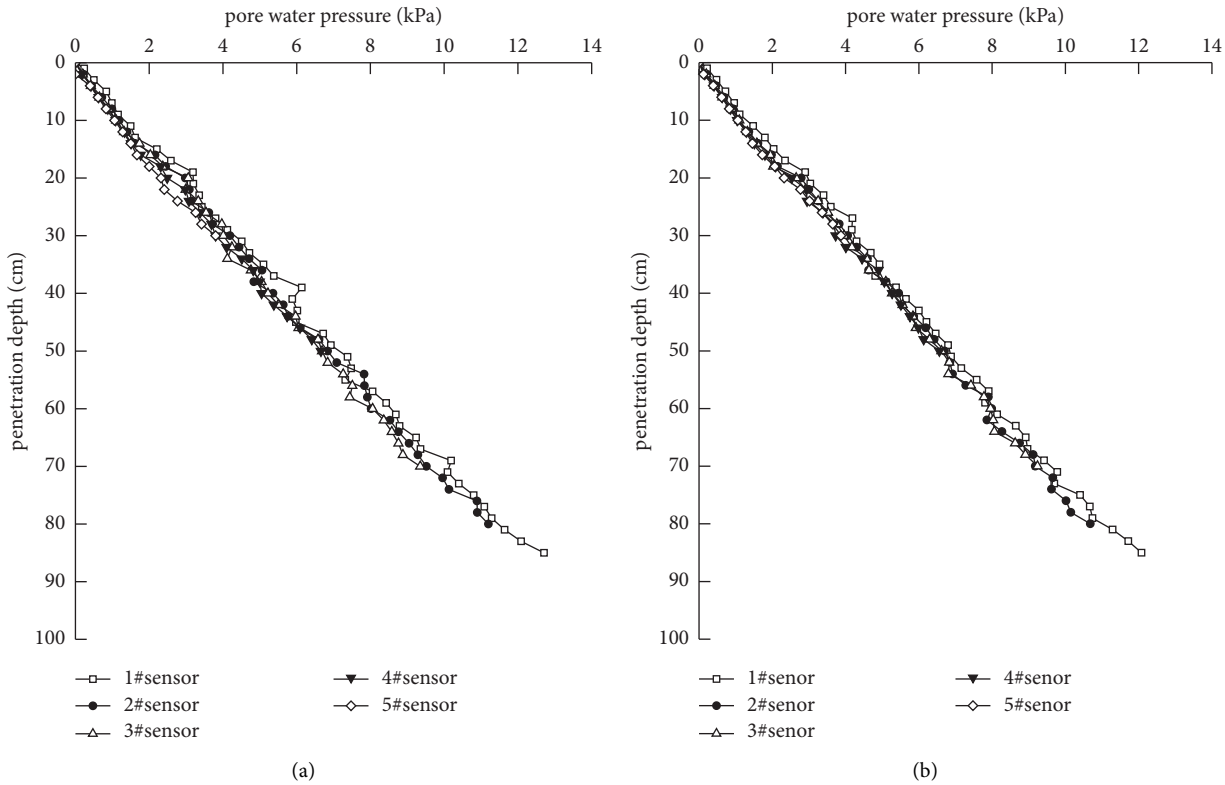

Figure 5: Distribution of test pile TP1 and TP2 pore water pressure during jacking. (a) TP1. (b) TP2.

Table 4: Ratio of excess pore water pressure at the pile-soil interface and overlying effective soil weight of test pile TP1.

Sensor station (h/L)	Excess pore water pressure (kPa)	Overlying effective soil weight (kPa)	Specific value (%)
1/20	4.21	6.88	61.2
1/10	3.2	5.76	55.6
1/5	2.35	4.64	50.6
2/5	1.66	3.52	47.2
3/5	0.79	2.4	32.9

Table 5: Table of ratio of excess pore water pressure at the pile-soil interface and overlying effective soil weight of test pile TP2.

Sensor station (h/L)	Excess pore water pressure (kPa)	Overlying effective soil weight (kPa)	Specific value (%)
1/20	3.58	6.88	52.1
1/10	2.68	5.76	46.5
1/5	2.24	4.64	48.3
2/5	1.56	3.52	44.3
3/5	0.87	2.4	36.3

soil, in shallow soil, ground rises, and valid stress can be drained upward, drainage conditions are good, and pore stress dissipates quickly. The pore stress of two test piles at this location quickly dissipates when the value of h/L is 3/5, and the surplus pore stress to valid soil weight ratio is only 32.9% and 36.3%.

3.1.3. Analysis of the Pile-Soil Interface's Radial Pressure. Figure 6 depicts the seismic forces as they were determined by the test piles TP1 and TP2's 1# × 5# earth pressure sensors as the piles sank. Figure 6 shows that as the pile sinks, the soil pressure steadily increases, which is consistent with Lehane's test results [11]. The horizontal earth pressure is minimal when the model pile's penetration depth is less than 10 cm and its growth rate is low, which is mainly because the long-term repeated shear effect as a result of the building pile sinking into the thin soil leads to a decrease of the cohesive force and a decrease of the contact tightness, resulting in a small lateral pressure. The radial earth pressure builds linearly and grows rapidly when the model pile's penetration

depth exceeds 10 cm. The closed-end test pile TP1 recorded radial earth pressures of 20, 03, 16, 68, 13, 23, 8, 42, and 5.1 kPa at the interface at the conclusion of sinking. The radial earth pressures corresponding to the open-end test pile TP2 were 19.59, 16.67, 13.83, 9.05, and 4.54 kPa, respectively. The vertical earth stress between the closed pile and the open pile is not significantly different, which can be seen from above. The radial earth stress rises in contact rises inversely with distance from pile end for both piles. The weight of the underlying soil has an influence on radial earth pressure, which explains why. A weaker squeeze causes a smaller increase in vertical earth stress because of the weight of covering clay soil with length from the heap end.

To explain the 'degradation' phenomenon of pile side soil pressure, the degradation value of adjacent sensors is marked with 'Δ' symbol in Figures 6(a) and 6(b). When the embedded depth is about 50 cm, the stress values of the adjacent sensors of the closed test pile TP1 are $\Delta_{1-2} = 2.08$ kPa, $\Delta_{2-3} = 1.51$ kPa, and $\Delta_{3-4} = 1.36$ kPa, respectively. Taking the opening test pile TP2 with a depth of 30 cm as an example, the lateral pressure degradation values of adjacent sensors are $\Delta_{1-2} = 1.36$ kPa, $\Delta_{2-3} = 1.0$ kPa, $\Delta_{3-4} = 0.92$ kPa, and $\Delta_{4-5} = 0.54$ kPa, respectively. According to the data above, at the same buried depth, the soil pressure degradation value steadily declines from the pile end to the pile top side. Radial earth pressure at the same depth exhibits a declining tendency as the pile sinking depth rises and the earth pressure "degenerates." The analysis was done because as the pile's depth increases, the soil surrounding it is continuously sheared, between both the stack and the soil, a mud-water film develops, there is less contact between the two, and the pressure is released.

3.1.4. Analysis of the Pile-Soil Interface's Effective Radial Pressure. The difference in functional earth stress and pore stress between both two test piles is seen in Figures 7 and 8, respectively. Figure 7 compares an increment of effective earth pressure and pore stress between TP1 and TP2, while Figure 8 demonstrates a similar situation. The effective stress is inversely correlated with the h/L value, however, the pore water pressure is greater than the actual earth pressure just at the stack interface. If the value of h/L is 9/10, the ratio of the effective soil stress and excess pore stress at the same place is 5.46 and 4.22 on TP1 and TP2 piles, respectively. The ratios at different h/L positions of the closed pile TP1 are 3.76, 4.2, 4.63, and 4.07, respectively, and the ratios at different h/L positions of the open pile TP2 are 4.47, 5.22, 5.17, and 4.8, respectively.

3.2. Static Load Test. Following pile jacking, the pressure test was run on test piles TP1 and TP2 with their ends open and closed, respectively. In this study, the closed-end test pile TP2 was first loaded. During the initial loading, the initial value of the load was too large, and the settlement was too large. The pore water pressure and soil pressure values are not the focus of this investigation. In this study, when the loading test of TP1 is carried out again. Throughout the loading process, the sensors monitor the pressures of pore water and earth pressure at various locations on the stack body.

3.2.1. Examination of the Pile-Soil Interface's Extra Pore Water Pressure Results. As the test is being loaded, Figure 8 displays the distribution of the test pile TP1's soil pore water pressure. The chart demonstrates that when the weight on the pile top is altered, the pore stress rises linearly and gradually as the pile depth gradually increases. Because of the load, the pore stress increasingly decreases throughout the length before gradually increasing to a relatively steady state. The pile is steadily sinking as the loading force rises, which will also cause pile deformation. The degree of the surrounding soil mass's compression is more visible the closer you get to the pile end. It is evident that the water pressure dissipation at the bottom is lower than at the top. The pile's interference with the surrounding soil and change in pore water pressure are both minimal when the pile is loaded. Besides, the sensor only measures the pore water pressure at a fixed depth using energy. Consequently, there is a clear linear trend in the reported pressure of the pore water distribution curve.

As seen in Figure 8, the pore stress of the underlying ground grows linearly with pile top load when the depth of penetration of the heap is in the same horizontal position. Both the top of the pile's weight and pore water pressure gradually increase. The water pressure does, however, vary very little at the start of loading and rapidly increases at the conclusion. According to the diagram, pile top loading will increase the soil's all pore water pressure when the residual soil is 85 cm deep. The pore water pressure increment values are 0.085 kPa, 0.032 kPa, 0.075 kPa, 0.108 kPa, 0.139 kPa, 0.122 kPa, 0.124 kPa, and 0.167 kPa, respectively, when the load increases from 1.4 kN to 7.0 kN. As can be observed, the water pressure value is higher at the top of the pile than it is at the bottom. This value will alter accordingly as the load changes, and the water pressure will rise as the weight increases. The explanation is that the deeper the force given to the pile top, the more obviously the soil is compressed, and the higher the pore stress will be in response. The sinking of piles happens dynamically. With the process of sinking, the size of the soil surrounding it determines its pressure, which will vary as well. Every loading process takes a while. Since the earth around the pile is essentially steady once the settlement is over, the water pressure there will also be essentially stable. The pile' top will be directly impacted by the load applied, which will subsequently have an effect on the soil and cause a rise in pore stress. The dirt surrounding the pile, however, is only being sheared with moderate power, the pore water pressure dissipates more slowly under low loads than it does under high loads because the surrounding soil is more stable under low loads. Under low loads, the pore water pressure value is higher. The increase is particularly noticeable when the pile top weight is between 6.3 kN and 7.0 kN because the soil surrounding the pile experiences intense shear action and pore stress rises quickly. The pore water stress showed an increasing trend with the penetration depth, which showed that with the

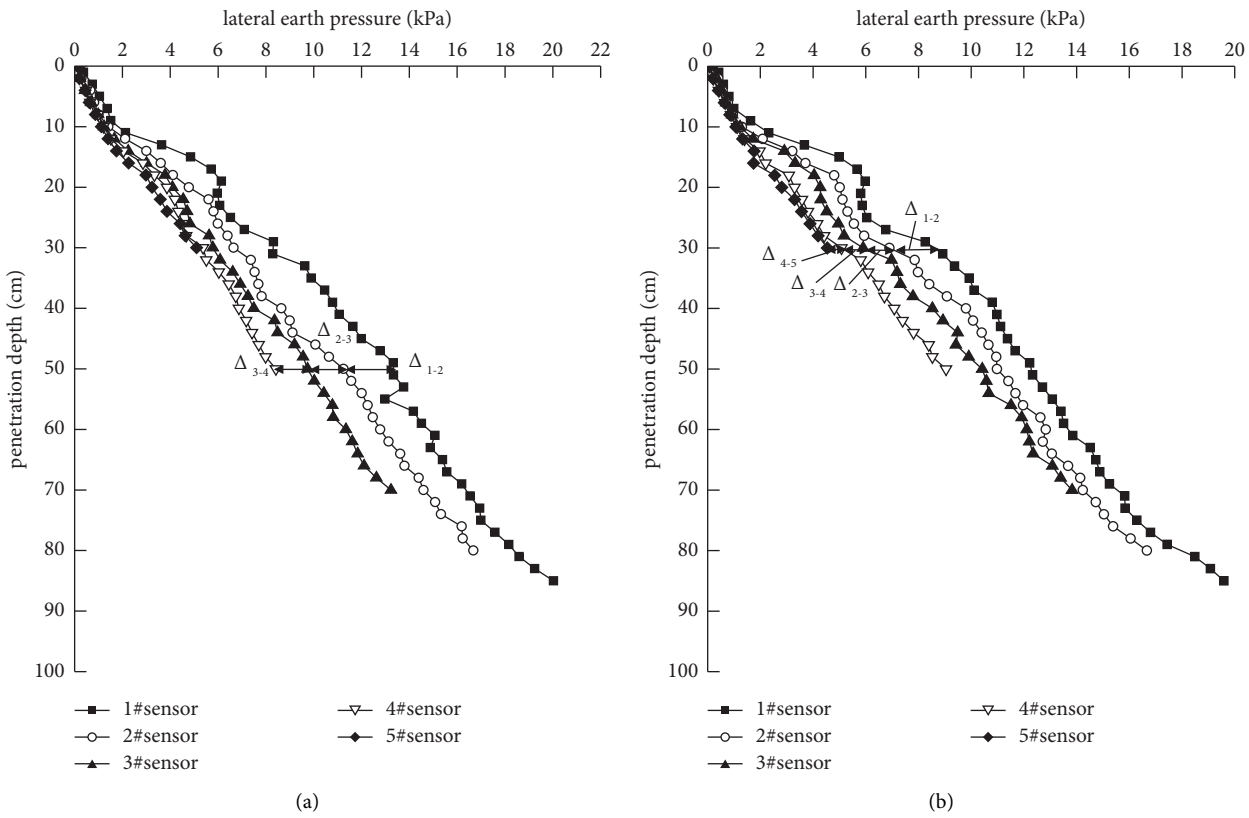

Figure 6: Distribution of effective radial pressure at the pile-soil interface of test piles TP1 and TP2 during the jacking process. (a) TP1. (b) TP2.

gradual exertion of the pile load transfer, the lager pile side stress, the lager adhesion between the pile soil, which was manifested as the gradual increase of pore stress.

Figure 9 displays the spread map of extra pore stress at the stack contact as determined by the exam pile TP1's pore pressure sensor during the loading operation. Figure 9 illustrates that under different loads applied to pile tops, the excess pore water pressure corresponding to different h/L positions increases with an increase in soil entry depth. When the top load is between 1.4 and 4.2 kN, the extra pore stress at different h/L positions increases approximately linearly following the pile. The extra pore stress grows roughly linearly between 0 and 80 cm of depth when the load exceeds 4.2 kN, whereas the slope of the curve slows between 80 and 85 cm of depth and the extra pore stress expresses a considerable upward trend. The reasons are as follows: after the pile top applied load exceeds 4.2 kN, the pile end and soil mass begin to produce relative displacement, and the extra pore water pressure greatly increases between 80 and 85 cm depth due to the strong extrusion pressure that the soil mass near the pile tip is subjected to an obvious soil mass impact at the bottom of the pile [18].

Additionally, Figure 9 shows that the load was between 1.4 and 7.0 kN after pile jacking was complete, and the final value, as determined by sensors placed at various h/L points, was between 0.6 and 1.46 kPa. Taking pile tip 1# sensor and pile tip 5# sensor as examples, under different load values applied on the pile tip, the increment amplitude of the 1# sensor is 0.6 kPa, 0.69 kPa, 0.72 kPa, 0.79 kPa, 0.9 kPa, 1.04 kPa, 1.16 kPa, 1.29 kPa, and 1.46 kPa, respectively. The increment amplitude of extra pore stress on the 5# sensor is 0.11 kPa, 0.12 kPa, 0.18 kPa, 0.21 kPa, 0.31 kPa, 0.4 kPa, 0.48 kPa, 0.55 kPa, and 0.63 kPa, respectively. As can be shown, the pile-soil interface experiences the largest surplus pore stress when the weight on the pile top is 7.0 kN. The extra pore stress produced by the 1# sensor and 5# sensor contact during the loading operation was 1.46 kPa and 0.63 kPa, respectively, which were both lower than the corresponding pressure at the end of the pile jacking, with a decrease of about 40.8% and 72.4%, respectively. The penetration test conducted by Lehane [11] in field clay soil showed that the radial pressure during static stability decreased to about 50% of the penetration time. It is close to the 40.8% and 72.4% obtained in this study. The reasons are as follows: Following the completion, the surplus pore stress diminishes, the earth's displacement is minimal, and the compaction is not immediately apparent. At the same time, it is clear that the increment amplitude of the pore stress rises with an increase in h/L and the increase is bigger the larger the load on the pile top.

3.2.2. Effective Radial Pressure Analysis of the Pile-Soil Interface. With the sinking of the pile, for the test pile TP1, radial pressure distribution at its interface changes linearly, and the specific curve is shown in Figure 10. The figure

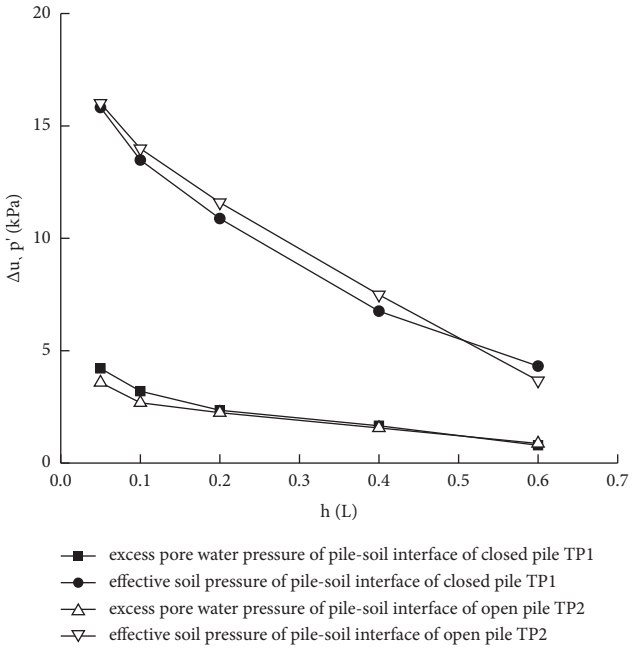

Figure 7: Comparison between effective soil pressure and excess pore water pressure at the pile-soil interface.

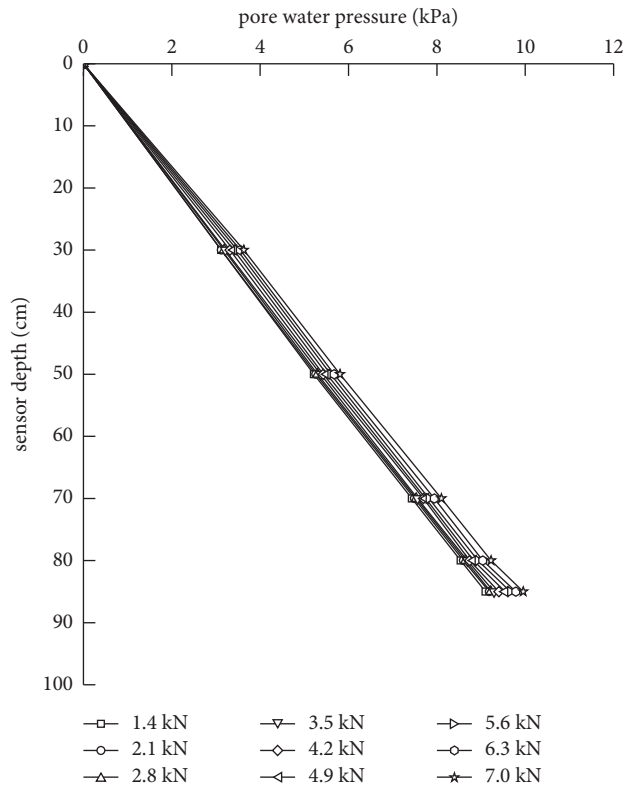

Figure 8: Distribution of pore water pressure of test pile TP1 during loading process.

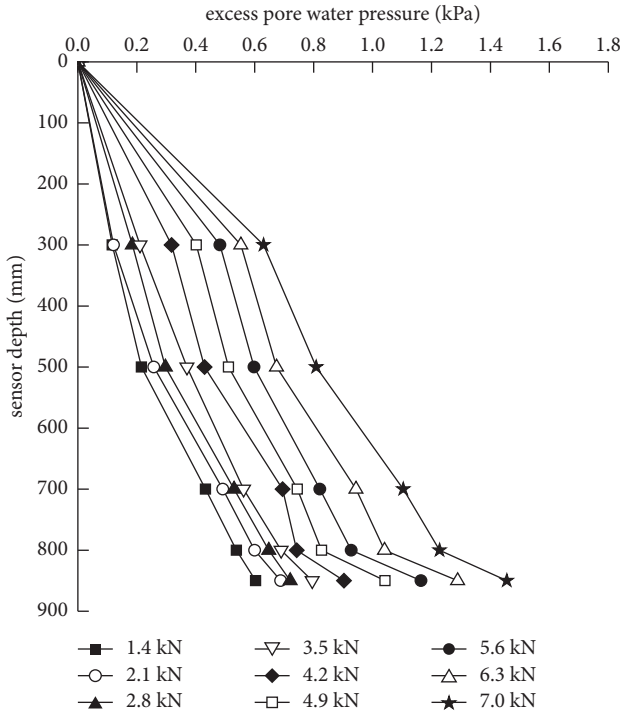

Figure 9: Distribution of excess pore water pressure in test pile TP1 during loading process.

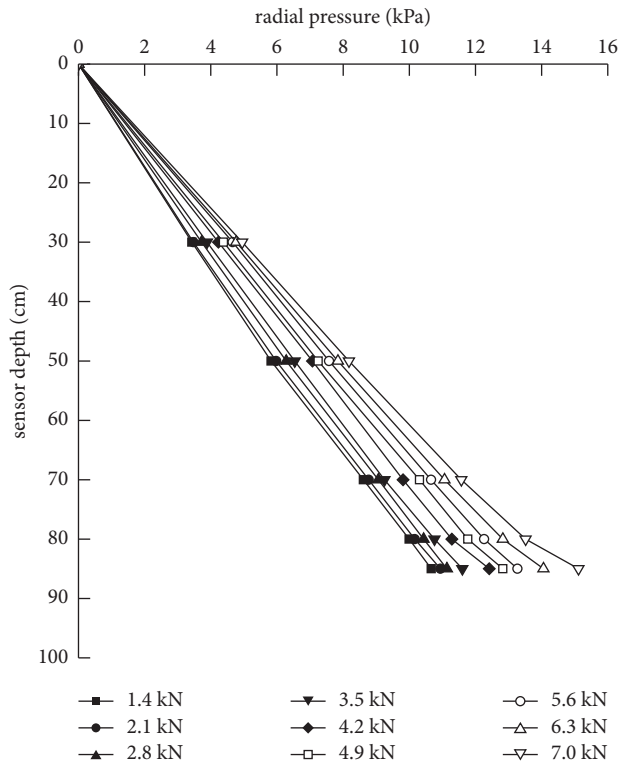

Figure 10: Distribution of radial pressure at the pile-soil interface of test pile TP1 during loading process.

demonstrates that the radial stress during the sinking process is lower than that of the pile during jacking. This is primarily due to the fact that the pile is less influenced by the load throughout loading and that the soil disturbance around the pile is less during loading than it is during jacking. Figure 10 indicates the variation of the radial stress

at the depth of the sensor under different loads. This is mostly due to the fact that the weight of the overburden increases with cover depth, increasing the radial stress between the pile and earth. The application of the weight to the pile top coincides with the pile's settlement. The initial load has a minor increment of radial pressure at the same depth. The increment of radial stress is rising along with the upper load's progressive growth. For example, when the load is between 6.3 kN and 7.0 kN, the change in its increment is more obvious, which is inconsistent with the variation rule of the vertical pressure during the jacking process. When the depth is 85 cm, the change in increment of radial pressure varies with the application of pile top load, which is 2.6%, 1.8%, 4.2%, 5.1%, 3.6%, 3.9%, 5.9%, and 7.5%, respectively. On the contrary, when the load becomes negative, the radial pressure changes significantly. The friction between the pile and soil is different from that during pile driving. During pile driving, the pile tip will disturb the surrounding soil greatly, resulting in continuous shear compression, which will gradually degrade the radial pressure. And because of the small deformation of the pile body in the process of loading and the long-time per level load, settlement stabilized, pile body balance formed a new gelling point of the pile and soil, the pile top load is small, so the small amount of settlement of the pile body and radial pressure caused by the subsidence growth is smaller and the radial pressure close to the static earth pressure [19]. The displacement variation between piles and soil is also changing, which causes the shear compression of the surrounding soil to also increase accordingly, increasing the radial pressure. The resolution increasingly rises with the rise load. For instance, the radial stress is at its highest when the loading amount is between 6.3 and 7.0 kN, which is the maximum loading amount. As a result, the surrounding soil's extrusion deformation is likewise the most noticeable.

The distribution of actual radial stress of TP1's pile-soil interface during loading is depicted in Figure 11. According to Figure 11, the pile-soil interface's efficient radial pressure is below the pile's effective radial pressure when the pile is loaded. Under different pile top load values, the pile-soil interface's effective radial pressure increases roughly linearly as the depth of the grave increases. At the same depth, the valid radial stress increases as the pile top load value increases [20]. Under different load values applied to pile tops, the effective radial pressure increment amplitude of the 1# sensor in the pile-soil interface was 10.06 kPa, 10.25 kPa, 10.42 kPa, 10.81 kPa, 11.51 kPa, 11.78 kPa, 12.11 kPa, 12.77 kPa, 13.66 kPa, respectively, and the increase was 1.0%, 2.0%, 3.8%, 6.5%, 2.6%, 2.5%, 5.8%, 7.0%, respectively. The effective radial pressure increment amplitude of the 5# sensor in pile-soil interface is 3.31 kPa, 3.35 kPa, 3.54 kPa, 3.67 kPa, 3.91 kPa, 3.98 kPa, 4.18 kPa, 4.22 kPa, and 4.32 kPa, respectively. The increment amplitude is 1.2%, 5.7%, 3.7%, 6.5%, 1.8%, 5.0%, 1.0%, and 2.4%, respectively. Under varing loads on the pile top, the increase in actual radial pressure contact as recorded by the two sensors is not greater than 10%. Pile top load value is 1.4~3.5 kN, the same depth of pile soil interface less effective radial pressure increase, pile top load value is 4.2~7.0 kN, pile-soil interface effective radial pressure increase, and at the top of the pile load values of 6.3 kN and 7.0 kN, pile top settlement increases obviously, the extrusion of the pile end is strong, and so the pile-soil interface of the pile end valid radial stress also has the obvious increasing trend, pile-soil interface effective radial pressure increment amplitude was 0.66 kPa, 0.89 kPa.

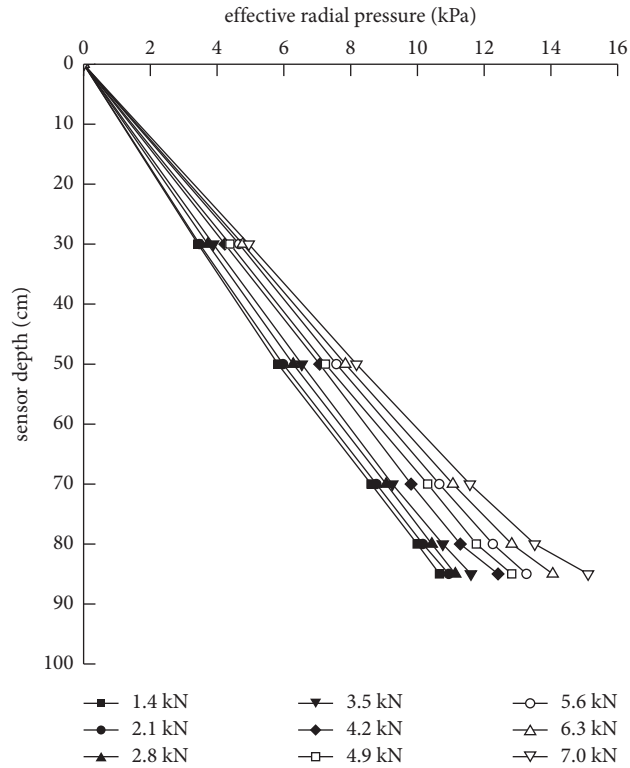

Figure 11: Distribution of effective radial pressure at the pile-soil interface of test pile TP1 during loading process penetration.

4. Conclusion

(1) As the sinking depth of the pile rises, the magnitude of extra pore stress and valid radial stress will also change accordingly, gradually increasing. When a pile reaches its maximum depth, the position of the h/L of the pile body will directly influence the magnitude of its increment. The larger the value of h/L, the smaller the incremental amplitude, while the incremental amplitude of a closed pile is larger than that of an open pile.

(2) The value of h/L has an inverse relationship with the valid radial stress at the same depth. The most severe radial pressure degradation occurs close to the pile top.

(3) The superstatic pore stress and valid radial stress during the pile sedimentation process and loading process are related to the position of h/L, so the length effect of the pile and the valid radial trust degradation need to be considered when settling and loading in the clay soil, so as not to overestimate the friction resistance on the pile side.

Data Availability

The data used to support the findings of this study are available from the corresponding author upon request.

Conflicts of Interest

The authors declare that they have no conflicts of interest regarding the publication of this study.

Authors' Contributions

Yonghong Wang and Xin Wang were responsible for conceptualized the study. Shiqiang Li and Jun Wang were responsible for data curation. Yonghong Wang was responsible for funding acquisition Lifeng Wang, Xunlong Niu, and Donglei Wang were responsible for project administration Yonghong Wang and Xin Wang were responsible for writing-original draft. Xin Wang and Yonghong Wang were responsible for writing-reviewing and editing.

Acknowledgments

This research was financially supported by the National Key R&D Program (2021YFE0113400) and the Shandong National Natural Science Foundation (ZR2022ME143).

References

[1] J. P. Carter, M. F. Randolph, and C. P. Wroth, "Stress and pore pressure changes in clay during and after the expansion of a cylindrical cavity," *International Journal for Numerical and Analytical Methods in Geomechanics*, vol. 3, no. 4, pp. 305–322, 1979.

[2] S. L. Shen, J. Han, H. H. Zhu, and Z. S. Hong, "Evaluation of a dike damaged by pile driving in soft clay," *Journal of Performance of Constructed Facilities*, vol. 19, no. 4, pp. 300–307, 2005.

[3] A. S. Vesic, "Expansion of cavities in infinite soil mass," *Journal of the Soil Mechanics and Foundations Division*, vol. 98, no. 3, pp. 265–290, 1972.

[4] M. M. Baligh, "Strain path method[J]," *J Geotech. Engng Div. Am. Soc. Civ.Engs*, vol. 111, pp. 1108–1136, 1985.

[5] A. J. Whittle and T. Sutabutr, "Prediction of pile setup in clay," *Transportation Research Record*, vol. 1663, no. 1, pp. 33–40, 1999.

[6] M. B. Chopra and G. F. Dargush, "Finite-element analysis of time-dependent large-deformation problems," *International Journal for Numerical and Analytical Methods in Geomechanics*, vol. 16, no. 2, pp. 101–130, 1992.

[7] L. F. Cao, C. I. Teh, and M. F. Chang, "Undrained cavity expansion in modified Cam clay I: theoretical analysis," *Géotechnique*, vol. 51, no. 4, pp. 323–334, 2001.

[8] F. S. Tehrani, F. Han, R. Salgado, and M. Prezzi, "Effect of surface roughness on the shaft resistance of non-displacement piles embedded in sand[J]," *Géotechnique*, vol. 66, no. 5, pp. 1–15, 2016.

[9] A. J. Bond and R. J. Jardine, "Effects of installing displacement piles in a high OCR clay," *Géotechnique*, vol. 41, no. 3, pp. 341–363, 1991.

[10] A. J. Bond and R. J. Jardine, "Shaft capacity of displacement piles in a high OCR clay," *Géotechnique*, vol. 45, no. 1, pp. 3–23, 1995.

[11] B. M. Lenane, *Experimental Investigations of Pile Behaviour Using Instrumental Field Piles [D]*, University of London (Imperial College), London, 1992.

[12] J. H. Hwang, N. Liang, and C. H. Chen, "Ground response during pile driving," *Journal of Geotechnical and Geo-Environmental Engineering*, vol. 127, no. 11, pp. 939–949, 2001.

[13] J. M. Pestana, C. E. Hunt, and J. D. Bray, "Soil deformation and excess pore pressure field around a closed-ended pile," *Journal of Geotechnical and GeoEnvironmental Engineering*, vol. 128, no. 1, pp. 1–12, 2002.

[14] The National Standards Compilation Group of People's Republic of China, *GB/T50123—1999 Standard for Soil Test method[S]*, China Planning Press, Beijing, 1999.

[15] Y. Y. Wang, S. K. Sang, M. Y. Zhang, D. S. Jeng, B. X. Yuan, and Z. X. Chen, "Laboratory study on pile jacking resistance of jacked pile," *Soil Dynamics and Earthquake Engineering*, vol. 154, Article ID 107070, 2022.

[16] Y. H. Wang, S. K. Sang, Y. F. Huang, M. Y. Zhang, D. Miao, and X. Y. Liu, "Model test of jacked pile penetration process considering influence of pile diameter[J]," *Frontiers in Physics*, vol. 9, Article ID 616410, 2021.

[17] J. Yang, L. G. Tham, P. K. K. Lee, and F. Yu, "Observed performance of long steel H-piles jacked into sandy soils," *Journal of Geotechnical and GeoEnvironmental Engineering*, vol. 132, no. 1, pp. 24–35, 2006.

[18] M. G. Iskander and R. E. Olsonl, *An Experimental Facility to Model the Behavior of Steel Pipe Piles in Sand*, The University of Texas at Austin, Austin, TX, USA, 1995.

[19] H. Liu, C. Zheng, X. Ding, and H. Qin, "Vertical dynamic response of a pipe pile in saturated soil layer," *Computers and Geotechnics*, vol. 61, pp. 57–66, 2014.

[20] R. D. Muhammed, J. Canou, J. C. Dupla, and A. Tabbagh, "Evaluation of local soil-pile friction in saturated clays under cyclic loading," *Soils and Foundations*, vol. 58, no. 6, pp. 1299–1312, 2018.